Supplementary Information Appendix for: A controller for walking derived from how humans recover from perturbations

Varun Joshi and Manoj Srinivasan
Mechanical and Aerospace Engineering
The Ohio State University, Columbus OH 43210 USA

The appendix contains the following sections:

- **Section S1** lists the equations of motion of the inverted pendulum biped model described in figure 1 of the main manuscript.

- **Section S2** provides specific information about the ODE solver and optimisation algorithms used in our calculations.

- **Section S3** provides information about the formal optimization problem to determine the controller for the inverted pendulum biped model.

- **Section S4** gives information about the perturbation impulses applied to the subjects and the resulting center of mass trajectories and velocities from the perturbation experiments.

- **Section S5** gives information about the variability and confidence intervals in the measured and inferred quantities, specifically, the center of mass state, foot placement, foot placement gains, and the mid-stance-to-mid-stance map.

- **Section S6** gives information about the goodness of fit for the derived controller

S1 Inverted pendulum walking: equations of motion

Body motion during single stance. The biped model is shown in figure S2 (figure 3 in the main text). See also [1,2] for a similar discussion. Positions in the lateral, forward and vertical directions are denoted by x, y, and z respectively, so that the center of mass position is $(x_\mathrm{com}, y_\mathrm{com}, z_\mathrm{com})$ and the foot position is $(x_\mathrm{foot}, y_\mathrm{foot}, z_\mathrm{foot})$. The equations of motion for the center of mass are:

$$m_\mathrm{com}\ddot{x}_\mathrm{com} \;=\; F\,\frac{x_\mathrm{com} - x_\mathrm{foot}}{\ell}, \tag{1}$$

$$m_\mathrm{com}\ddot{y}_\mathrm{com} \;=\; F\,\frac{y_\mathrm{com} - y_\mathrm{foot}}{\ell}, \text{ and} \tag{2}$$

$$m_\mathrm{com}\ddot{z}_\mathrm{com} \;=\; F\,\frac{z_\mathrm{com} - z_\mathrm{foot}}{\ell} - m_\mathrm{com}g. \tag{3}$$

where F is the force along the leg and ℓ is leg length, given by:

$$\ell^2 = \left(x_\mathrm{com} - x_\mathrm{foot}\right)^2 + \left(y_\mathrm{com} - y_\mathrm{foot}\right)^2 + \left(z_\mathrm{com} - z_\mathrm{foot}\right)^2. \tag{4}$$

a) Histogram of backwards perturbations

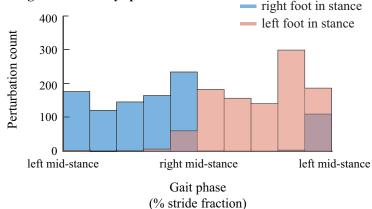**b) Histogram of sideways perturbations**

Figure S1: Phase of impulses applied during perturbation experiment. For each perturbed step, we looked at the forces applied at the pelvis for the 0.5s before the mid-stance for a "highly perturbed" step. For these force, the instance where the force was maximum was noted to be the phase of the applied perturbation. This figure shows a histogram of phases for a) the backwards perturbation experiment, and b) the sideways perturbation experiment. In each of the figures, the horizontal axis represents bins of 10% phase each, starting and ending with left mid-stance. The vertical axis counts the number of perturbations in each bin. The blue filled boxes correspond to steps where the right leg was in stance, thus the perturbing forces considered occur in the 0.5 s before the right mid-stance. The red filled boxes correspond to steps where the left leg was in stance, thus the perturbing forces considered occur in the 0.5 s before the left mid-stance.

This leg length ℓ is a constant during the inverted pendulum single stance: $\ell = \ell_{max}$. The equality constraint along with the previous differential equations gives a set of "differential algebraic equations". We convert the algebraic constraint $\ell = \ell_{max}$ into the second order ODE $\ddot{\ell} = 0$, which can be solved along with the other equations for the center-of-mass accelerations and the required leg-force to keep the leg length constant, allowing a forward integration given an initial biped state. While this integration may not, by itself, ensure leg length constancy, the constancy of leg length is enforced in the optimization (described in section S2 below) as a constraint on the initial values of the leg length and leg length rate: $\ell = \ell_{max}$ and $\dot{\ell} = 0$ at the beginning of each stance phase.

Effect of an impulse. Push-off and heel-strike impulses are collisional [3], in that they result in an instantaneous change in the body velocity. When an impulse I acts along the leg, the change in the
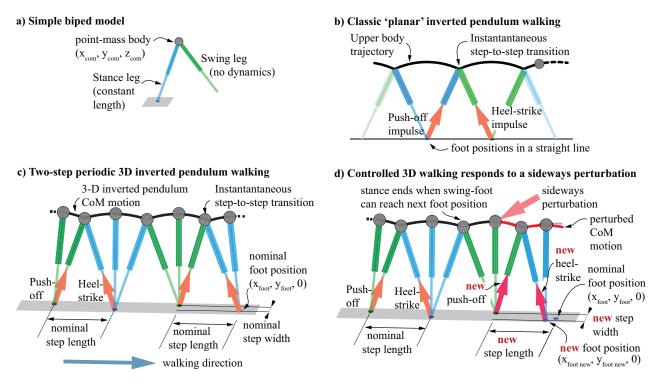
Figure S2: Inverted pendulum walking with a simple biped. a) This biped consists of a point-mass and two mass-less legs. The inverted pendulum walking gait consists of single-stance inverted-pendulum motions separated by an instantaneous step-to-step transition consisting of a push-off and a heel-strike impulse along the trailing and leading legs. b) The classic inverted pendulum walking gait is planar, with the inverted pendulum motions being planar and the foot placements along a line. c) The 3D inverted pendulum walking motion consists of 3D inverted pendulum phases, and the foot placements not in a line. A two-step periodic 3D inverted pendulum walking motion is shown. d) The 3D inverted pendulum walking motion can be controlled by modulating the next target foot-position and the applied push-off impulse, allowing the biped to recover from perturbations. This figure contains elements from figure 3 of the main manuscript.

body center of mass velocity is given by:

$$\Delta m_{\mathrm{com}} \dot{x}_{\mathrm{com}} = I\, \frac{x_{\mathrm{com}} - x_{\mathrm{foot}}}{\ell}, \tag{5}$$

$$\Delta m_{\mathrm{com}} \dot{y}_{\mathrm{com}} = I\, \frac{y_{\mathrm{com}} - y_{\mathrm{foot}}}{\ell}, \text{ and} \tag{6}$$

$$\Delta m_{\mathrm{com}} \dot{z}_{\mathrm{com}} = I\, \frac{z_{\mathrm{com}} - z_{\mathrm{foot}}}{\ell}. \tag{7}$$

These equations are used directly to compute the consequences of a given push-off impulse. To solve for the heel-strike impulse, we use these equations in addition to the condition that the leg length rate after the collision is zero.

Non-dimensionalization. All variables were non-dimensionalized using mass m_{com}, leg length ℓ_{max}, and acceleration due to gravity g. Here are some examples: non-dimensional forward position $\bar{y}_{\mathrm{com}} = y_{\mathrm{com}}/\ell_{\mathrm{max}}$, non-dimensional leg force $\bar{F} = F/(m_{\mathrm{com}}g)$, non-dimensional speed $\bar{v} = v/\sqrt{g\ell_{\mathrm{max}}}$, and non-dimensional time $\bar{t} = t\sqrt{g/\ell_{\mathrm{max}}}$, where the overbar denotes the non-dimensional variant of the variable.

S2 Inverted pendulum walking: nominal motion and forward simulation

Problem formulation. The nominal motion for the biped was determined by determining the unique two-step periodic inverted pendulum walking motion with a given step period t_{step}, step width w_{step}, the step length d_{step}. We use a shooting-like method to determine such a motion. See also [1, 4, 5].

Specifically, knowing the equations of motion, we can simulate each step of the inverted pendulum motion by defining the duration of each step, namely $t_{\text{step},1}$ and $t_{\text{step},2}$, the initial position and velocity of the center of mass for the first step, namely $(x_{\text{com10}}, y_{\text{com10}}, z_{\text{com10}})$ and $(\dot{x}_{\text{com10}}, \dot{y}_{\text{com10}}, \dot{z}_{\text{com10}})$, the initial position and velocity of the center of mass for the second step, namely $(x_{\text{com20}}, y_{\text{com20}}, z_{\text{com20}})$ and $(\dot{x}_{\text{com20}}, \dot{y}_{\text{com20}}, \dot{z}_{\text{com20}})$, the scalar values of the four impulses along the leg, namely $I_{\text{push}-\text{off1}}$, $I_{\text{heel}-\text{strike1}}$, $I_{\text{push}-\text{off2}}$ and $I_{\text{heel}-\text{strike2}}$, and the locations of the feet for the two steps, namely $(x_{\text{foot1}}, y_{\text{foot1}})$ and $(x_{\text{foot,2}}, y_{\text{foot,2}})$.

Without loss of generality, the position of the foot for the first step is fixed to the origin for the system. The position of the foot for the second step is determined by the given step-width and step-length from the experiments, and the step periods are also set to match data from our experiments. These constraints leaves us 16 unknown variables to determine: $\mathbb{Z} = ($ x_{com10}, y_{com10}, z_{com10}, $\dot{x}_{\text{com10}}$, $\dot{y}_{\text{com10}}$, $\dot{z}_{\text{com10}}$, x_{com20}, y_{com20}, z_{com20}, $\dot{x}_{\text{com20}}$, $\dot{y}_{\text{com20}}$, $\dot{z}_{\text{com20}}$, $I_{\text{push}-\text{off1}}$, $I_{\text{heel}-\text{strike1}}$, $I_{\text{push}-\text{off2}}$, $I_{\text{heel}-\text{strike2}})$.

Each step is simulated independently and starts with a heel-strike impulse that ensures that the leg-length-rate after impulse is exactly zero. We then integrate the smooth equations of motion forward in time for the duration of the step period. Then, a push-off impulse is applied.

The unknown variable $\mathbb{Z}$ is determined so as to satisfy the following constraints: (1) Inequality constraints to prevent negative impulses (the foot pulling on the ground): $0 \leq I_j$; (2) An equality constraint on the initial leg length for each step: $\ell = \ell_{\text{max}}$. (3) Continuity constraints ensuring that the state at the end of the first step is equal to the state at the beginning of the second step; that is, $x_{\text{com}}\left(t_{\text{step}}\right) = x_{\text{com20}}$, $y_{\text{com}}\left(t_{\text{step}}\right) = y_{\text{com20}}$, $z_{\text{com}}\left(t_{\text{step}}\right) = z_{\text{com20}}$, $\dot{x}_{\text{com}}\left(t_{\text{step}}\right) = \dot{x}_{\text{com20}}$, $\dot{y}_{\text{com}}\left(t_{\text{step}}\right) = \dot{y}_{\text{com20}}$, $\dot{z}_{\text{com}}\left(t_{\text{step}}\right) = \dot{z}_{\text{com20}}$, $z_{\text{platform}}\left(t_{\text{step}}\right) = z_{\text{platform20}}$, and $\dot{z}_{\text{paltform}}\left(t_{\text{step}}\right) = \dot{z}_{\text{platform20}}$. (4) Periodicity constraints ensuring that the state at the end of the second step is equal to the state at the beginning of the first step except for a forward translation. $x_{\text{com}}\left(2t_{\text{step}}\right) = x_{\text{com10}}$, $y_{\text{com}}\left(2t_{\text{step}}\right) = y_{\text{com10}} + 2d_{\text{step}}$, $z_{\text{com}}\left(2t_{\text{step}}\right) = z_{\text{com10}}$, $\dot{x}_{\text{com}}\left(2t_{\text{step}}\right) = \dot{x}_{\text{com10}}$, $\dot{y}_{\text{com}}\left(2t_{\text{step}}\right) = \dot{y}_{\text{com10}}$ and $\dot{z}_{\text{com}}\left(2t_{\text{step}}\right) = \dot{z}_{\text{com10}}$.

Computational methods. We used `ode45` in `MATLAB` with absolute and relative tolerances of 10^{-9} for integrating the differential equations in forward simulations. To determine the biped's nominal motion, we used the nonlinear optimiser `SNOPT` [6, 7] with default feasibility tolerances of 10^{-6} to determine the unknown $\mathbb{Z}$ consistent with the constraints above.

The equality constraint equations above are such that there is a locally unique solution that satisfies all of them. That is, the number of equations is equal to the number of unknowns (with the linearization of the equations having full rank). We use a optimization algorithm to solve this 'root finding' problem only because we can conveniently impose inequality constraints such as positivity of push-off impulse and forward progression of the biped. The optimization has a dummy constant objective function equal to 1, so the results only depend on the constraints. Repeated optimizations converged to the same results, providing some numerical evidence for global uniqueness of the obtained motion.

S3 Inverted pendulum walking: optimization to fit the controller

Formulation of the optimization problem. In the main text, we describe the process of calculating the mid-stance-to-mid-stance state map J_1 as well as the foot-placement map K from human data. We also describe how these maps are symmeterized about the sagittal plane. For the simulated biped the

mid-stance-to-mid-stance state map can be written as

$$\Delta \begin{bmatrix} X_{\text{CoM}}(n+1) \\ \dot{X}_{\text{CoM}}(n+1) \\ \dot{Y}_{\text{CoM}}(n+1) \end{bmatrix}_{\text{mid-stance}} = (J_2 + J_3 \cdot J_4) \cdot \Delta \begin{bmatrix} X_{\text{CoM}}(n) \\ \dot{X}_{\text{CoM}}(n) \\ \dot{Y}_{\text{CoM}}(n) \end{bmatrix}_{\text{mid-stance}} . \tag{8}$$

In this equation J_2 and J_3 are properties of the biped model. J_4 represents the set of nine independent free variables for the system. Of these, $J_4(1:2,:)$ is the foot placement controller and $J_4(3,:)$ is the impulse controller. These free parameters are what we use to make the inverted pendulum biped behave in a human-like manner.

In practice we have 18 parameters, 9 for left-to-right steps ($J_{4_{\text{left to right}}}$) and 9 for right-to-left steps ($J_{4_{\text{right to left}}}$), and 9 constraints that ensure symmetry about the sagittal plane. For the controller $J_{4_{\text{left to right}}}$, we simulate the inverted pendulum biped for 1 step and determine the mid-stance-to-mid-stance state map J_1^*. We then generate a set of 15 error terms :

$$e = \begin{bmatrix} J_4(1,1) - K(1,1) \\ J_4(1,2) - K(1,2) \\ J_4(1,3) - K(1,3) \\ J_4(2,1) - K(1,1) \\ J_4(2,2) - K(2,2) \\ J_4(2,3) - K(2,3) \\ J_1^*(1,1) - J_1(1,1) \\ J_1^*(1,2) - J_1(1,2) \\ J_1^*(1,3) - J_1(1,3) \\ J_1^*(2,1) - J_1(2,1) \\ J_1^*(2,2) - J_1(2,2) \\ J_1^*(2,3) - J_1(2,3) \\ J_1^*(3,1) - J_1(3,1) \\ J_1^*(3,2) - J_1(3,2) \\ J_1^*(3,3) - J_1(3,3) \end{bmatrix} .$$

The optimization problem can be written as:

$$\underset{J_4}{\text{minimize}} \quad f_0(J_4),$$

$$\text{subject to} \quad f_1(J_4) = 0,$$

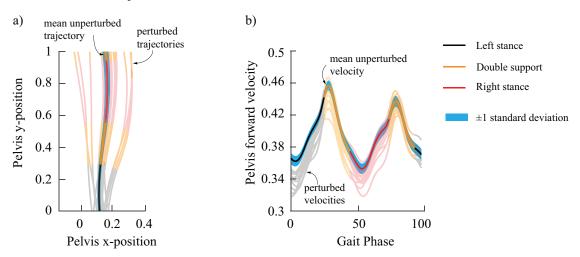where

$$f_0(J_4) = \Sigma_{i=1}^{15}(\lambda_i e_i)^2$$

and

$$f_1(J_4) = \begin{bmatrix} J_{4_{\text{left to right}}}(1,1) - J_{4_{\text{right to left}}}(1,1) \\ J_{4_{\text{left to right}}}(1,2) - J_{4_{\text{right to left}}}(1,2) \\ J_{4_{\text{left to right}}}(1,3) + J_{4_{\text{right to left}}}(1,3) \\ J_{4_{\text{left to right}}}(2,1) + J_{4_{\text{right to left}}}(2,1) \\ J_{4_{\text{left to right}}}(2,2) + J_{4_{\text{right to left}}}(2,2) \\ J_{4_{\text{left to right}}}(2,3) - J_{4_{\text{right to left}}}(2,3) \\ J_{4_{\text{left to right}}}(3,1) + J_{4_{\text{right to left}}}(3,1) \\ J_{4_{\text{left to right}}}(3,2) + J_{4_{\text{right to left}}}(3,2) \\ J_{4_{\text{left to right}}}(3,3) - J_{4_{\text{right to left}}}(3,3) \end{bmatrix} .$$

Here, λ_i is a scaling parameter equal to the inverse of the confidence interval for the corresponding human derived data. Details of these confidence intervals can be found in section S5.

S4   Experimental details

Perturbation phase.   The perturbing forces in our experiments were applied by humans pulling on cables magnetically connected to a belt tied around the pelvis of the subjects. These forces ranged in duration from 0.5s - 0.9s and were thus much longer duration than those typically found in experiments using robots to pull on subjects [8, 9]. Figure S1 shows a histogram of perturbation phases corresponding to forces applied before each "highly perturbed" step (as defined in the main text) from a) the backward and b) the sideways perturbation experiments. The phase for the perturbing force was determined by looking at the peak applied force for a duration of 0.5s preceding each mid-stance corresponding to the "highly perturbed" step. The blue filled boxes correspond to steps where the right leg was in stance, thus the perturbing forces considered occur in the 0.5 s before the right mid-stance. The red filled boxes correspond to steps where the left leg was in stance, thus the perturbing forces considered occur in the 0.5 s before the left mid-stance.

Human response to perturbations.   Figure S3 shows the center of mass response to perturbations in "highly perturbed" steps (as defined in the main text) for strides starting with a left mid-stance in both, the sideways and backward, perturbation experiments. Examples of these perturbations are used in the main text while trying to recreate human behaviour using the simulated biped. For the sideways experiment we picked example trajectories that have both a rightwards position and rightwards velocity deviation at mid-stance as these are far more distinct from the mean unperturbed trajectory than other combinations, i.e. leftward velocity deviation with rightward position deviation, rightward velocity deviation with leftward position deviations.

More recoveries from perturbations

Figure S3: Pelvis position and velocity trajectories from experiment. a) Top view of center of mass position trajectories for "highly perturbed" steps from one trial in the sideways perturbation experiment. b) Pelvis forward velocity for "highly perturbed" steps from one trial in the backward perturbation experiment. Each trajectory corresponds to different mid-stance state deviation magnitudes, the darker line represents the mean "unperturbed" motion with the blue band around it marking ±1 standard deviation around the mean motion. These strides all start with a left mid-stance; two complete steps (one stride) are shown.

S5 Variability in the human data

Mid-stance pelvis state variability. The subject's state at each mid-stance is slightly different, and this is also true for the highly perturbed steps. The standard deviation for the non-dimensionalized states of all subjects for these highly perturbed steps are as follows:

$$\sigma_{X_{\text{pelvis}}} = 0.03 \text{ for left to right steps and } 0.03 \text{ for right to left steps,}$$

$$\sigma_{\dot{X}_{\text{pelvis}}} = 0.03 \text{ for left to right steps and } 0.03 \text{ for right to left steps, and}$$

$$\sigma_{\dot{Y}_{\text{pelvis}}} = 0.02 \text{ for left to right steps and } 0.02 \text{ for right to left steps.}$$

The covariance matrix for the non-dimensionalized states of all subjects for perturbed left to right steps is given by:

$$\text{cov}(\Delta X_{\text{pelvis}}, \Delta \dot{X}_{\text{pelvis}}, \Delta \dot{Y}_{\text{pelvis}}) = 10^{-3} \cdot \begin{bmatrix} 0.81 & -0.07 & 0.05 \\ -0.07 & 0.78 & 0.10 \\ 0.05 & 0.10 & 0.52 \end{bmatrix},$$

with eigenvalues $(0.47 \cdot 10^{-3}, 0.77 \cdot 10^{-3}, 0.87 \cdot 10^{-3})$. For right to left steps, this matrix is given by:

$$\text{cov}(\Delta X_{\text{pelvis}}, \Delta \dot{X}_{\text{pelvis}}, \Delta \dot{Y}_{\text{pelvis}}) = 10^{-3} \cdot \begin{bmatrix} 0.96 & -0.19 & -0.02 \\ -0.19 & 0.78 & -0.04 \\ -0.02 & -0.04 & 0.57 \end{bmatrix},$$

with eigenvalues $(0.54 \cdot 10^{-3}, 0.68 \cdot 10^{-3}, 1.08 \cdot 10^{-3})$. All three eigenvalues being comparable in magnitude, and none of them being too small compared to the others, means that this three-dimensional data cannot be reduced to two. The mid-stance state variability during the unperturbed steps along with the limits of the basin of attraction are shown in Table S1.

Table S1: Standard deviation of states in normal (unperturbed) walking for the backward (AP) and the medio-lateral (ML) protocols and maximum perturbations for which the controlled biped simulation remains stable.

State	AP exp	ML exp	Basin max/min limits
X_{pelvis}	0.0100	0.0119	0.25/-0.21
$\dot{X}_{\text{pelvis}}$	0.0084	0.0083	0.26/-0.20
$\dot{Y}_{\text{pelvis}}$	0.0075	0.0084	0.35/-0.19

Foot-placement variability. The standard deviations for the non-dimensionalized foot-positions of all subjects for perturbed steps are as follows:

$$\sigma_{X_{\text{foot}}} = 0.08 \text{ for left to right steps and } 0.07 \text{ for right to left steps, } and$$

$$\sigma_{Y_{\text{foot}}} = 0.06 \text{ for left to right steps and } 0.05 \text{ for right to left steps.}$$

The covariance matrix for the non-dimensionalized foot-placement deviations of all subjects for perturbed left to right steps is given by:

$$\text{cov}(\Delta X_{\text{foot}}, \Delta Y_{\text{foot}}) = 10^{-2} \cdot \begin{bmatrix} 0.68 & -0.10 \\ -0.10 & 0.32 \end{bmatrix}$$

with eigenvalues $(0.30 \cdot 10^{-2}, 0.71 \cdot 10^{-2})$. For right to left steps, this matrix is given by:

$$\text{cov}(\Delta X_{\text{foot}}, \Delta Y_{\text{foot}}) = 10^{-2} \cdot \begin{bmatrix} 0.54 & 0.13 \\ 0.13 & 0.28 \end{bmatrix}$$

with eigenvalues $(0.22 \cdot 10^{-2}, 0.59 \cdot 10^{-2})$.

Foot placement gain variability. The foot placement relationship derived directly from human data, as shown in section 3 of the main text, is the symmetrized version of two different relationships, one each for the set of steps for which the left foot and right foot are in stance. The 95% confidence interval for the linear relationship derived from steps in left stance is:

$$\Delta X_{\text{foot}} = (1.93 \pm 0.04) \cdot \Delta X_{\text{pelvis}} + (2.07 \pm 0.04) \cdot \Delta \dot{X}_{\text{pelvis}} + (0.04 \pm 0.05) \cdot \Delta \dot{Y}_{\text{pelvis}} \text{ and}$$

$$\Delta Y_{\text{foot}} = -(0.40 \pm 0.07) \cdot \Delta X_{\text{pelvis}} - (0.97 \pm 0.07) \cdot \Delta \dot{X}_{\text{pelvis}} + (0.84 \pm 0.08) \cdot \Delta \dot{Y}_{\text{pelvis}}.$$

The 95% confidence interval for the linear relationship derived from steps in right stance is:

$$\Delta X_{\text{foot}} = (1.78 \pm 0.04) \cdot \Delta X_{\text{pelvis}} + (1.84 \pm 0.04) \cdot \Delta \dot{X}_{\text{pelvis}} - (0.11 \pm 0.05) \cdot \Delta \dot{Y}_{\text{pelvis}} \text{ and}$$

$$\Delta Y_{\text{foot}} = (0.54 \pm 0.05) \cdot \Delta X_{\text{pelvis}} + (1.10 \pm 0.06) \cdot \Delta \dot{X}_{\text{pelvis}} + (0.77 \pm 0.06) \cdot \Delta \dot{Y}_{\text{pelvis}}.$$

Mid-stance-to-mid-stance map variability. The left-to-right mid-stance-to-mid-stance map J_1, along with the 95% confidence interval is given by:

$$J_1 = \begin{bmatrix} -(0.40 \pm 0.03) & -(0.92 \pm 0.03) & -(0.06 \pm 0.04) \\ (0.42 \pm 0.02) & (0.36 \pm 0.02) & -(0.11 \pm 0.02) \\ -(0.04 \pm 0.02) & -(0.16 \pm 0.02) & (0.27 \pm 0.02) \end{bmatrix} \text{ with } R^2 = \begin{bmatrix} 0.62 \\ 0.56 \\ 0.22 \end{bmatrix}.$$

The right-to-left mid-stance-to-mid-stance map with its 95% confidence interval is given by:

$$J_1 = \begin{bmatrix} -(0.33 \pm 0.03) & -(0.79 \pm 0.03) & (0.07 \pm 0.03) \\ (0.39 \pm 0.02) & (0.32 \pm 0.02) & (0.07 \pm 0.02) \\ (0.08 \pm 0.02) & (0.18 \pm 0.02) & (0.27 \pm 0.02) \end{bmatrix} \text{ with } R^2 = \begin{bmatrix} 0.55 \\ 0.50 \\ 0.30 \end{bmatrix}.$$

Variability in individual gains. The foot-placement gains and the mid-stance-to-mid-stance map can be fit for each individual subject as well. Figures S4 and S5 show the variability of these fits for left-to-right and right-to-left steps respectively. The gains for the main diagonal elements of J_1 and each of the foot-placement gains for each subject are color coded. The box-plot shows the median of this distribution, a 25% to 75% confidence interval box, and whiskers corresponding to 2.5 times the standard deviation. Outliers are marked with a red cross. The black dot shows the mean of the pooled data that is used in the controller derivation.
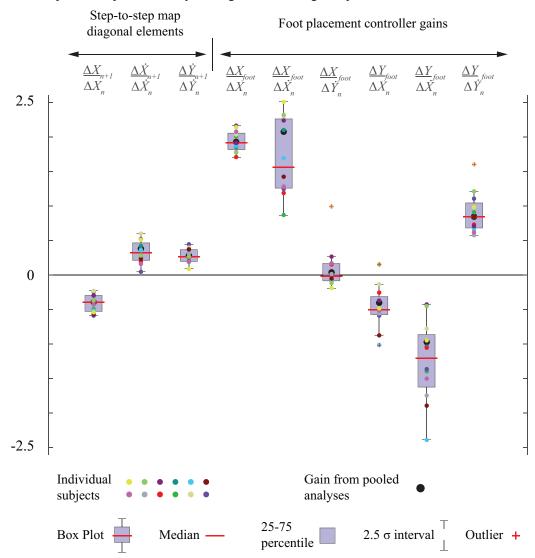
S6 Accuracy of the controller fit

Residuals for the controller fits. The fitting of the inverted pendulum model to the human-derived foot placement and step to step maps resulted in small non-zero residuals. Specifically, the residuals for the foot placement controller were:

$$e_1 = \begin{bmatrix} 0.21 & 0.27 & -0.34 \\ -0.07 & -0.02 & 0.17 \end{bmatrix}$$

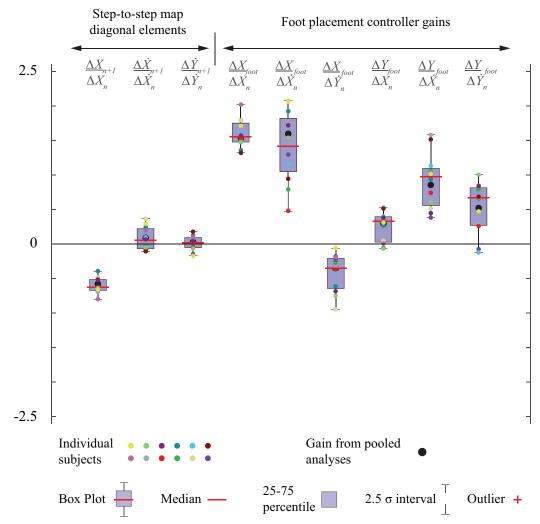and the residuals for the symmetrized left to right Poincaré map were

$$e_2 = \begin{bmatrix} -0.03 & -0.005 & -0.06 \\ -0.02 & -0.02 & 0.14 \\ 0.01 & 0.01 & -0.06 \end{bmatrix}.$$

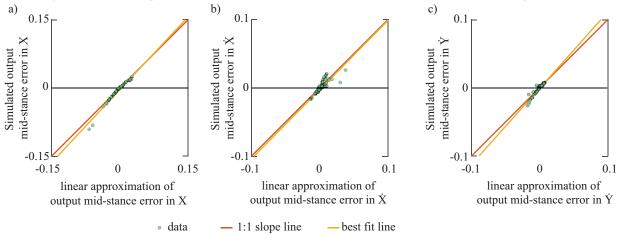Subject-to-subject variability in the gains: Left to right steps

Step-to-step map
diagonal elements

Foot placement controller gains

$\dfrac{\Delta X_{n+1}}{\Delta X_n}$ $\dfrac{\Delta \dot{X}_{n+1}}{\Delta \dot{X}_n}$ $\dfrac{\Delta \dot{Y}_{n+1}}{\Delta \dot{Y}_n}$ $\dfrac{\Delta X_{foot}}{\Delta X_n}$ $\dfrac{\Delta X_{foot}}{\Delta \dot{X}_n}$ $\dfrac{\Delta X_{foot}}{\Delta \dot{Y}_n}$ $\dfrac{\Delta Y_{foot}}{\Delta X_n}$ $\dfrac{\Delta Y_{foot}}{\Delta \dot{X}_n}$ $\dfrac{\Delta Y_{foot}}{\Delta \dot{Y}_n}$

2.5

0

-2.5

Individual subjects

Gain from pooled analyses

Box Plot   Median —   25-75 percentile   2.5 σ interval   Outlier +

Figure S4: Variability in individual gains. The mid-stance-to-mid-stance gains and foot-placement gains can be derived for each individual subject. The gains for the main diagonal elements of J_1 and each of the foot-placement gains for each subject are color coded. The box-plot shows the median of this distribution, a 25 - 75 percentile box, and whiskers corresponding to 2.5 σ. Outliers are marked with a red cross. The black dot shows the mean of the pooled data that is used in the controller derivation. These strides all start with a left mid-stance.

The controlled inverted pendulum biped produces a close, but not perfect, approximation of the human center of mass dynamics. Figure S6 shows a comparison of mid-stance state errors in the next step, i.e. the 2nd step after perturbations, as predicted by the mid-stance-to-mid-stance J_1 (on the horizontal axis) and the simulated biped (on the vertical axis). The green dots represent one of a 100 randomly sampled input peturbations from the experimental data. The yellow line shows the best fit to this data. If the center of mass dynamics of the simulated biped perfectly matched the mid-stance-to-mid-stance map J_1, then this best fit line would exactly overlap the red line.

Figure S5: Variability in individual gains. The mid-stance-to-mid-stance gains and foot-placement gains can be derived for each individual subjects. The gains for the main diagonal elements of J_1 and each of the foot-placement gains for each subject are color coded. The box-plot shows the median of this distribution, a 25 - 75 percentile box, and whiskers corresponding to 2.5 σ. The black dot shows the mean of the pooled data that is used in the controller derivation. These strides all start with a right mid-stance.

Predicting state after one step: Three-D model simulations versus linear mid-stance-to-mid-stance map

Figure S6: Full 3D simulation versus linear model. Comparing state deviations one step after a perturbed step, as predicted by using full 3D simulation versus as predicted by the linear mid-stance-to-mid-stance map. For illustrative purposes, we only display 100 randomly selected data points, whereas the best-fit line is fit to the full data set.
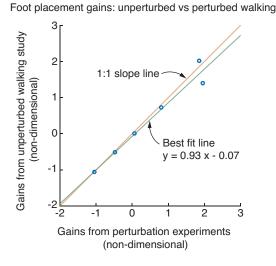

Figure S7: Unperturbed walking vs perturbed walking. The foot placement gains inferred from the perturbation experiments herein (horizontal axis) are quantitatively similar to those derived from unperturbed walking (vertical axis) in a previous study [10]. The similarity two sets of gains is characterized by the best fit line $y = 0.93x - 0.07$, with an $R^2 = 0.963$. It appears that the largest relative difference in the gains is in the response of sideways foot placement X_{foot} to deviations in mid-stance $\dot{X}_{\text{pelvis}}$. Dropping this gain in the comparison gives an $R^2 = 0.996$ and a regression equation $y = 1.05x - 0.03$. Note that the gains from [10] have been non-dimensionalized here for direct comparison.

References

[1] Joshi V, Srinivasan M. Walking on a moving surface: energy-optimal walking motions on a shaky bridge and a shaking treadmill can reduce energy costs below normal. Proc Roy Soc A. 2015;471:20140662.

[2] Joshi V, Srinivasan M. Walking crowds on a shaky surface: Stable walkers discover Millennium Bridge oscillations with and without pedestrian synchrony. Biology Letters. 2018;14:20180564.

[3] Ruina A, Bertram JE, Srinivasan M. A collisional model of the energetic cost of support work qualitatively explains leg sequencing in walking and galloping, pseudo-elastic leg behavior in running and the walk-to-run transition. Journal of theoretical biology. 2005;237(2):170–192.

[4] Srinivasan M, Ruina A. Computer optimization of a minimal biped model discovers walking and running. Nature. 2006;439:72–75.

[5] Srinivasan M. Fifteen observations on the structure of energy minimizing gaits in many simple biped models. J Roy Soc Interface. 2011;8:74–98.

[6] Gill PE, Murray W, Saunders MA. SNOPT: An SQP algorithm for large-scale constrained optimization. SIAM review. 2005;47(1):99–131.

[7] Holmström K. The TOMLAB optimization environment in Matlab. 1999;.

[8] Hof AL, Vermerris SM, Gjaltema WA. Balance responses to lateral perturbations in human treadmill walking. J Exp Biol. 2010;213:2655–2664.

[9] Vlutters M, Van Asseldonk EH, Van der Kooij H. Center of mass velocity-based predictions in balance recovery following pelvis perturbations during human walking. Journal of experimental biology. 2016;219(10):1514–1523.

[10] Wang Y, Srinivasan M. Stepping in the direction of the fall: the next foot placement can be predicted from current upper body state in steady-state walking. Biology letters. 2014;10:20140405.